Expansion Dynamics of Interacting Bosons in Homogeneous Lattices in One and Two Dimensions

J. P. Ronzheimer,[1,2] M. Schreiber,[1,2] S. Braun,[1,2] S. S. Hodgman,[1,2] S. Langer,[3,4] I. P. McCulloch,[5] F. Heidrich-Meisner,[3,6] I. Bloch,[1,2] and U. Schneider[1,2]

[1]*Department of Physics, Ludwig-Maximilians-Universität München, 80799 München, Germany*
[2]*Max-Planck-Institut für Quantenoptik, 85748 Garching, Germany*
[3]*Department of Physics and Arnold Sommerfeld Center for Theoretical Physics, Ludwig-Maximilians-Universität München, 80333 München, Germany*
[4]*Department of Physics and Astronomy, University of Pittsburgh, Pittsburgh, Pennsylvania 15213, USA*
[5]*Centre for Engineered Quantum Systems, School of Mathematics and Physics, The University of Queensland, St. Lucia, QLD 4072, Australia*
[6]*Friedrich-Alexander Universität Erlangen-Nürnberg, Institut für Theoretische Physik II, 91058 Erlangen, Germany*

(Received 23 January 2013; published 13 May 2013)

We experimentally and numerically investigate the expansion of initially localized ultracold bosons in homogeneous one- and two-dimensional optical lattices. We find that both dimensionality and interaction strength crucially influence these nonequilibrium dynamics. While the atoms expand ballistically in all integrable limits, deviations from these limits dramatically suppress the expansion and lead to the appearance of almost bimodal cloud shapes, indicating diffusive dynamics in the center surrounded by ballistic wings. For strongly interacting bosons, we observe a dimensional crossover of the dynamics from ballistic in the one-dimensional hard-core case to diffusive in two dimensions, as well as a similar crossover when higher occupancies are introduced into the system.

DOI: 10.1103/PhysRevLett.110.205301 PACS numbers: 67.85.−d, 05.30.Jp, 37.10.Jk

Nonequilibrium dynamics of strongly correlated many-body systems pose one of the most challenging problems for theoretical physics [1]. Especially in one dimension, many fundamental questions concerning transport properties and relaxation dynamics in isolated systems remain under active debate. These problems have attracted a renewed interest in recent years due to the advent of ultracold atomic gases. The ability to control various system parameters in real time has not only allowed quantum simulations of equilibrium properties of interacting many-body systems [2], but has also enabled experimental studies of quantum quenches [3–7] and particle transport [8–12] in clean, well-controlled, and isolated systems. Here, we study the combined effects of interactions and dimensionality on the expansion dynamics of bosonic atoms in optical lattices.

While interactions generally lead to diffusive transport in higher dimensions, the situation is more involved in one dimension, where the phase space available for scattering can be severely limited. This was demonstrated, for example, by the experimental realization of a quantum Newton's cradle [5], showing that not all 1D Bose gases thermalize (see also Ref. [13]). An intriguing phenomenon in one dimension is the existence of an exact mapping [14] from hard-core bosons on a lattice or a Tonks-Girardeau gas [15,16] to noninteracting spinless fermions, demonstrating the integrability of these systems. Furthermore, this mapping establishes that the time evolution of the density distribution is identical for hard-core bosons and noninteracting fermions. As a consequence, hard-core bosons in one dimension expand ballistically and, asymptotically, undergo a dynamical fermionization during the expansion [17,18]. In a transient regime, even initial 1D Mott insulators with unity filling are predicted to become coherent during the expansion and to dynamically form long-lived quasicondensates at finite momenta [19–21]. In the presence of doubly occupied lattice sites (doublons) or even higher occupancies, the above mapping is not applicable. The dynamics then become more involved and can include intriguing quantum distillation effects, namely a demixing of doublons and single atoms [22,23].

Several powerful theoretical methods have been used to study the expansion dynamics in one dimension, including the time-dependent density matrix renormalization group method (t-DMRG) (see, e.g., Refs. [20,22,24]) and approaches based on the existence of exact solutions (see, e.g., Refs. [25–29]). For interacting 2D systems, in contrast, one needs to resort to approximate methods such as the time-dependent Gutzwiller ansatz, which predicts dynamical condensation even in two dimensions [30,31].

In this work, we experimentally study the expansion of initially localized bosonic atoms in the lowest band of an optical lattice. We investigate how the expansion speed changes as a function of interaction strength and how it is affected by the dimensionality of the system. Furthermore, we identify the role of multiply occupied lattice sites in the system and compare our results to t-DMRG [32–34] calculations in the 1D case.

Experimental sequence.—The experiment starts with a Bose-Einstein condensate of approximately 10^5 bosonic

^{39}K atoms in a three-beam optical dipole trap. The condensate is loaded into a blue-detuned, three-dimensional optical lattice (lattice constant $d = \lambda/2$, wavelength $\lambda = 736.7$ nm) with a lattice depth of $V_0 = 33.0(5)E_r$. Here, $E_r = h^2/(2m\lambda^2)$ denotes the recoil energy, m the atomic mass, and h is Planck's constant. For suitable harmonic confinements, sufficiently strong repulsive interactions, and adiabatic loading, a large Mott insulating core with unity filling and a radius of (40–50) d is created in the center [see Fig. 1(a)]. By employing a Feshbach resonance at a magnetic field of 402.50(3) G we can tune the interaction strength during loading and thereby control the amount of multiply occupied lattice sites. In the deep lattice, where tunneling is suppressed [tunneling time $\tau_d = \hbar/J_d \approx 58$ ms, with the tunneling amplitude J_d and $\hbar = h/(2\pi)$], the atoms are held for a 20 ms dephasing period, during which any residual coherences between lattice sites are lost [35] and all atoms become localized to individual lattice sites. The resulting state after this loading procedure is a product of local Fock states, $|\Psi_{\text{initial}}\rangle = \prod_i \frac{1}{\sqrt{\eta_i!}}(\hat{b}_i^\dagger)^{\eta_i}|0\rangle$, $\eta_i \in \{0, 1, 2, \ldots\}$, where $\hat{b}_i^\dagger$ is the creation operator for a boson on site i. This state is characterized by a flat quasimomentum distribution $n_k = \text{const}$, where $k \in [-\pi/d, \pi/d]$ denotes the quasimomentum. During the dephasing period, we change the magnetic field to set the desired interaction strength U/J for the expansion. Because of the suppressed hopping during this part of the sequence, this field ramp does not alter the density distribution; i.e., the initial state prior to the expansion is identical for all interactions. The expansion is initiated by lowering the lattice depth along one or both horizontal directions (x, y) in 150 μs to a depth of 8.0(1) E_r to induce tunneling with amplitudes J_x ($\tau = \hbar/J_x = 0.55$ ms) and J_y between neighboring lattice sites along these directions. This is equivalent to a quantum quench from $U/J \approx \infty$ to a finite U/J. Simultaneously, the strength of the dipole trap is reduced to a small but finite value that compensates the anti-confinement along the expansion direction created by the lattice beams (see Ref. [36] for Supplemental Material).

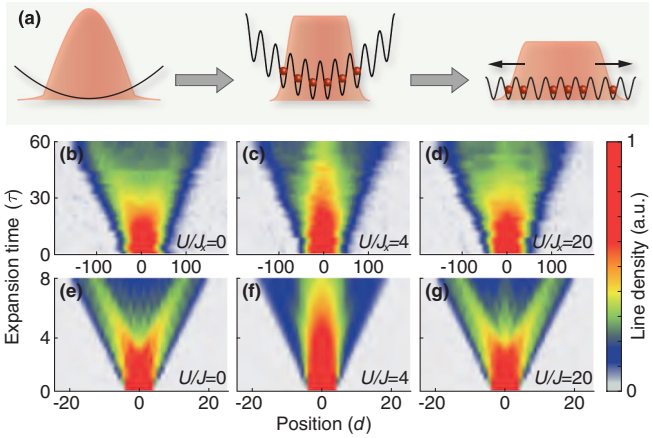

FIG. 1 (color). Experimental sequence and time evolution during the expansion. (a) Sketch of the experimental sequence. (b)–(d) Experimental time evolution of line density profiles during a 1D expansion for various interaction strengths (each line is individually normalized). (e)–(g) Corresponding t-DMRG calculations for eight atoms, plotted using cubic interpolation.

The dynamics in the resulting lattice can be described within the homogeneous Bose-Hubbard model:

$$H = -J_x \sum_{\langle i,j\rangle_x} \hat{b}_i^\dagger \hat{b}_j - J_y \sum_{\langle i,j\rangle_y} \hat{b}_i^\dagger \hat{b}_j + \frac{U}{2}\sum_i \hat{n}_i(\hat{n}_i - 1).$$

Here, U denotes the on-site interaction strength, $\hat{n}_i = \hat{b}_i^\dagger \hat{b}_i$, and $\langle i, j\rangle_{x(y)}$ indicates a summation over nearest neighbors along the x (y) direction.

We monitor the *in situ* density distribution of the expanding cloud using standard absorption imaging along the vertical axis. The recorded column densities are integrated over one direction and the resulting line densities are presented in Figs. 1(b)–1(d) as a function of the expansion time for the 1D case. In both the noninteracting and the hard-core limits we expect a ballistic expansion which splits the cloud into a left- and right-moving portion [20,37,38], as can be seen in our numerical results shown in Figs. 1(e) and 1(g). While the splitting can be clearly observed in the experimental data for the noninteracting case [Fig. 1(b)], the presence of a few multiply occupied lattice sites decreases its visibility in the strongly interacting case [Fig. 1(d)].

Expansion velocities.—To quantify the expansion dynamics we extract the half-width-at-half-maximum (HWHM) from the line density profiles [39] and determine the core expansion velocities v_c [Fig. 2(a)] via linear fits to the evolution of the HWHM at intermediate times [36]. In both one and two dimensions, the maximum core expansion velocity occurs in the noninteracting limit, where the system expands ballistically. Because of an exact dynamical symmetry of Hubbard models on bipartite lattices, the expansion dynamics are independent of the sign of the interaction [40] and we therefore focus the discussion on the $U > 0$ case. In two dimensions, increasing the interaction strength monotonically reduces the core expansion velocity until it essentially drops to zero. In one dimension, in contrast, a similar but much weaker suppression of the expansion velocity extends only up to interaction strengths on the order of the bandwidth $U \sim 4J_x$, while v_c increases again for stronger interactions and eventually reaches values comparable to the noninteracting case.

The same qualitative behavior is evident in the t-DMRG simulations for ten particles, shown as red triangles in Fig. 2(a). Since the numerically calculated HWHM suffers from rather large finite-size effects, we also present t-DMRG results for an alternative measure of the expansion velocity, namely $v_r = (d/dt)\sqrt{R^2(t) - R^2(0)}$, extracted from the radius $R^2(t) = (1/N)\sum_i \langle \hat{n}_i(t)\rangle (i - i_0)^2 d^2$ (inset),

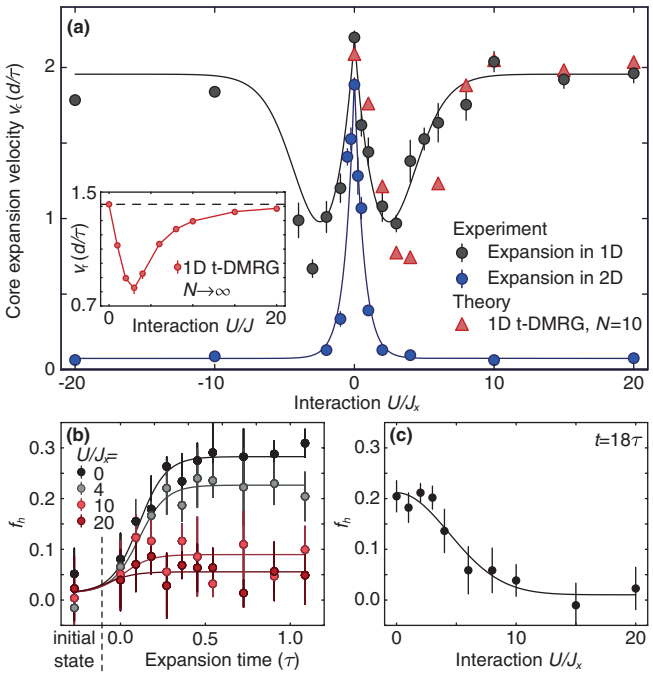

FIG. 2 (color). Core expansion velocity and dynamical generation of higher occupancies. (a) Core expansion velocity v_c for experimental data in one dimension (black circles, lattice depth (8, 33, 33) E_r along (x, y, z), $J_y \approx 0$) and two dimensions (blue circles, (8, 8, 33) E_r, $J_x = J_y$) and t-DMRG calculations for $N = 10$ particles in one dimension (red triangles). Experimental error bars denote the standard deviation of the linear fits. Inset: v_r calculated by t-DMRG and extrapolated to infinite particle number. Error bars are given by the uncertainty of the extrapolation [36]. (b) Higher occupancy, as measured by f_h, versus expansion time in the experiment. For the points labeled "initial state", the measurement was performed directly after the dephasing period in the deep lattice [36]. (c) f_h after an expansion time of $t = 18\tau$. Error bars in (b) and (c) show standard deviations of averaging four data points. All lines are guides to the eye.

where N is the particle number and i_0 denotes the central lattice site. It is more robust against finite-size effects and allows an extrapolation to infinite particle number [36], and, in our setup, exhibits the same qualitative dependence on U. Moreover, at $U = 0$, v_r has an intuitive physical interpretation, as it is in this case equal to the average expansion velocity v_{av}. The latter is given by the initial quasimomentum distribution through $v_{\mathrm{av}} = 1/(N\hbar)\sqrt{\sum_k (\partial\epsilon_k/\partial k)^2 n_k}$, where $\epsilon_k = -2J\cos(kd)$ denotes the tight-binding dispersion relation. For the given initial state, where n_k is flat, this results in $v_{\mathrm{av}} = \sqrt{2}(d/\tau)$, illustrated by the dashed line in the inset of Fig. 2(a). Usually, one would associate a constant velocity with a ballistic expansion and would expect $\sqrt{R^2(t) - R^2(0)} \propto \sqrt{t}$ for diffusive dynamics. In the case of the sudden expansion, however, the interpretation is more complicated, because the diffusion constant is density dependent and the density distribution is inhomogeneous and time-dependent (see Refs. [11,37] for details).

The fast expansion for strong interactions in 1D is a consequence of the system entering into the hard-core boson regime, where, at $U = \infty$, it can be exactly mapped to noninteracting fermions, which expand ballistically with $v_r = \sqrt{2}(d/\tau)$ [36]. Even though hard-core bosons undergo collisions and their quasimomentum distribution changes over time [19,20], the above mapping guarantees that the evolution of their density distribution is ballistic and identical to the noninteracting case. In other words, the conservation of the quasimomentum distribution of the underlying noninteracting fermions severely constrains the scattering processes, thereby preventing the dynamics from becoming diffusive.

Starting from the hard-core boson limit, the decrease of the expansion velocity towards smaller interactions can be qualitatively understood by considering the dynamical formation of doublons and higher occupancies. For $U/J \gtrsim 4$, isolated doublons in one dimension can be thought of as heavy compound objects, propagating with typical effective hopping matrix elements on the order of J^2/U [41]. While their formation is energetically suppressed at $U/J \gg 4$, for smaller U the system can maximize its local entropy through the formation of doublons (and higher occupancies) during the early phase of the expansion [see Figs. 2(b) and 2(c)]. Therefore, as U decreases, higher occupancies begin to form and the expansion velocity decreases. In addition, the possibility of creating higher occupancies increases the phase space available for scattering and therefore favors diffusive dynamics. For vanishing interactions, the scattering cross section approaches zero and the expansion becomes ballistic again with a large velocity of $v_r = \sqrt{2}(d/\tau)$. Therefore, there has to be a minimum of v_c at some intermediate U, which turns out to be close to the critical $U/J \approx 3.4$ for the 1D Mott insulator to superfluid transition [42]. This is consistent with other studies of quantum quenches, which observe the fastest relaxation times close to the critical point [7,43].

The buildup of higher occupancies during the initial expansion dynamics shown in Fig. 2(b) is monitored by comparing the number of atoms left after a parity projection N_{par} with the total atom number N_{total}, yielding $f_h = (N_{\mathrm{total}} - N_{\mathrm{par}})/N_{\mathrm{total}}$. In the absence of triply or higher occupied sites, f_h measures the fraction of atoms on doubly occupied sites [36]. While the expansion starts from an initial state with essentially no higher occupancy, f_h rises significantly over roughly the first half tunneling time. After this initial buildup, f_h remains almost constant and changes only on the much slower time scale of the expansion [compare Fig. 2(c)]. This initial fast relaxation is purely local, as can be seen in t-DMRG calculations comparing the relaxation timescale to the evolution of the system without opening the trap [36]. The formation of

higher occupancies is accompanied by changes in n_k and results in an increase of interaction energy and therefore a decrease in kinetic energy. The effect of the reduced kinetic energy (as measured by v_{av}) is, however, much smaller than the observed reduction of the expansion velocity [36]. We thus conclude that scattering processes during the expansion are mainly responsible for the slower expansion.

1D-2D crossover.—In Fig. 3 we analyze how the expansion dynamics change when we gradually tune the dimensionality from a purely 1D system towards a 2D geometry. This is implemented by varying the depth of the lattice along the y direction and thereby the tunneling ratio $\chi = J_y/J_x$ for the expansion [44]. Upon increasing χ, the expansion dynamics at strong interactions change fundamentally. Instead of the fast expansion observed in the 1D case [Fig. 3(a)], the major fraction of the cloud simply remains in the center [Fig. 3(c)]. Moreover, the column density profiles shown in the insets of Fig. 3(d) exhibit a characteristic bimodal structure. In the 2D case, this structure consists of a slowly expanding, round, diffusive core on top of a square-shaped ballistic background and can be seen for all moderate to strong interactions. In one dimension, on the other hand, a similar behavior is only visible for intermediate interaction strengths.

In Fig. 3(d), we illustrate how the interaction dependence of v_c changes as we go from a 1D system with two integrable limits to a 2D system, where only the noninteracting case is integrable. The expansion speed in the noninteracting case is independent of χ, since in this case the dynamics along the two lattice axes are separable. For all values of χ, the expansion speed initially decreases with increasing interactions. For small χ, the core expansion velocity increases again for strong interactions, whereas, for $\chi > 0.5$, it remains minimal. The behavior at large χ, as well as the bimodal cloud shape, is analogous to the dynamics of strongly interacting lattice fermions in two dimensions, which were shown to be diffusive [11]. The square-shaped background consists of ballistically expanding atoms originating from the edge of the high density core, while collisions render the expansion diffusive for atoms inside the core. Such diffusive dynamics are consistent with the numerical observation that hard-core bosons in two dimensions thermalize [45]. Our experimental results show a qualitative difference between the dynamics in one and two dimensions in the strongly interacting regime, whereas theoretical studies using the time-dependent Gutzwiller ansatz predict a qualitatively similar behavior, independent of dimension [30,31,46]. Overall, we observe that, for interacting systems, the expansion along one direction is suppressed by an increased tunneling along a transverse direction. This promotes the notion that increasing transverse tunneling enlarges the accessible phase space for scattering processes and therefore favors diffusive dynamics.

Higher occupancies in the initial state.—Figure 4 illustrates the effect of a random admixture of higher occupancies in the initial state on the expansion dynamics. This admixture is created by loading the lattice at smaller interaction strength and higher densities, such that no clear Mott insulator will form. Nonetheless, the dephasing in the deep lattice remains effective, such that the initial state of the expansion can still be described as a product of local Fock states, but with higher occupancies on some

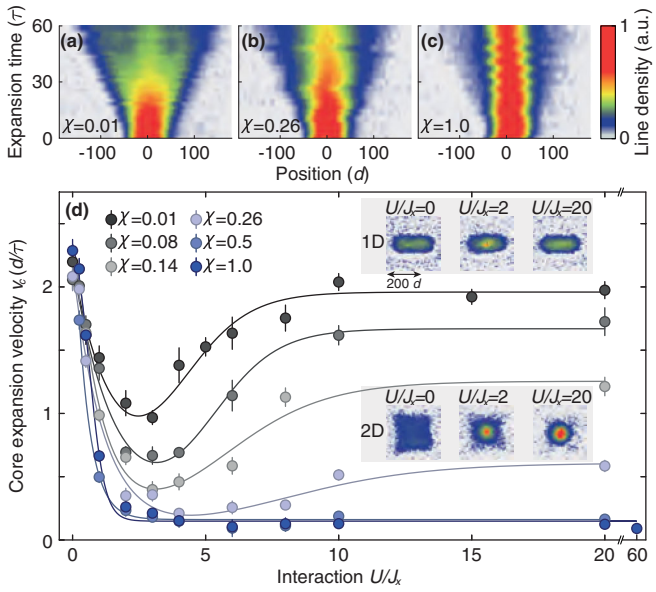

FIG. 3 (color). 1D-2D crossover. (a)–(c) Evolution of line density profiles for various tunneling ratios $\chi = J_y/J_x$ and $U/J_x = 10$. (d) Experimental core expansion velocity v_c for various χ. Lines are guides to the eye. Error bars denote the standard deviation of the linear fits. The insets show the column density at $t \approx 36\tau$.

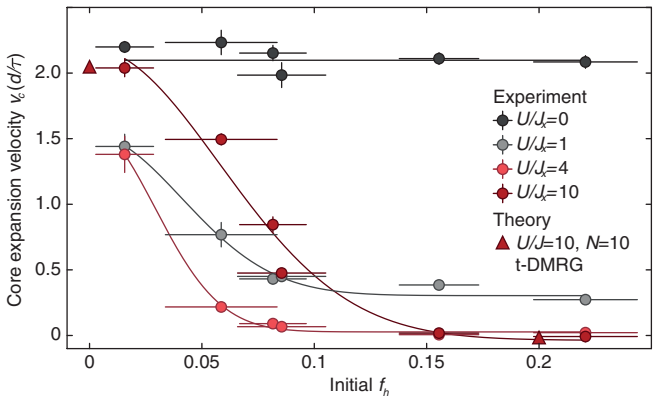

FIG. 4 (color). Effect of higher occupancies in the initial state. Core expansion velocity v_c in one dimension as a function of the higher occupancy, as measured by f_h, in the initial state for various interaction strengths. Solid lines are guides to the eye. Vertical error bars show the standard deviation of the linear fits, horizontal error bars the standard deviation of averaging 16 measurements.

randomly chosen sites. While there is, as expected, no significant effect of multiply occupied sites in the noninteracting case, where each atom expands individually, already at $U/J_x = 1$ higher occupancies in the initial state reduce the core expansion velocity. This reduction becomes most dramatic close to the hard-core limit ($U/J_x = 10$), where the originally high expansion velocity quickly approaches zero. In this limit, any higher occupancies are long-lived [47] and their small effective higher-order tunneling rate slows down the expansion [22,24]. Furthermore, the presence of multiply occupied lattice sites in the strongly interacting limit can give rise to quantum distillation processes [22] and, thereby, the formation of a stable core of doubly occupied lattice sites [48].

Conclusion.—Experimentally, we find the fastest expansions near the exactly solvable limits of the Bose-Hubbard model, where additional conservation laws restrict scattering such that diffusion is not possible. These are (i) the noninteracting limit, irrespective of dimension, and (ii) the case of infinitely strong interactions in one dimension, provided there are no higher occupancies in the initial state. Deviations from these cases, either by finite interactions, the crossover towards two dimensions, or an admixture of higher occupancies in the initial state, lead to a substantial suppression of the expansion. In the case of the crossover to two dimensions at large U/J, the emergence of diffusive dynamics in the core is additionally signaled by the characteristic bimodal cloud shape previously observed in the fermionic case [11]. In one dimension at intermediate interactions or with initially multiply occupied lattice sites, both experimental and t-DMRG profiles suggest an almost bimodal structure here as well. Therefore, we conjecture that the common reason for the slow expansions seen in the experiments is the emergence of diffusive dynamics in the core region of the cloud.

We thank Daniel Garbe and Tim Rom for their contributions in constructing the experimental apparatus and Lode Pollet, Marcos Rigol, Achim Rosch, and Julia Wernsdorfer for insightful discussions. We acknowledge financial support from the Deutsche Forschungsgemeinschaft (FOR801, FOR912, Deutsch-Israelisches Kooperationsprojekt Quantum phases of ultracold atoms in optical lattices), the US Defense Advanced Research Projects Agency (Optical Lattice Emulator program), and Nanosystems Initiative Munich.

[1] A. Polkovnikov, K. Sengupta, A. Silva, and M. Vengalattore, Rev. Mod. Phys. **83**, 863 (2011).
[2] I. Bloch, J. Dalibard, and W. Zwerger, Rev. Mod. Phys. **80**, 885 (2008).
[3] M. Greiner, O. Mandel, T. Hänsch, and I. Bloch, Nature (London) **419**, 51 (2002).
[4] L. E. Sadler, J. M. Higbie, S. R. Leslie, M. Vengalattore, and D. M. Stamper-Kurn, Nature (London) **443**, 312 (2006).
[5] T. Kinoshita, T. Wenger, and D. S. Weiss, Nature (London) **440**, 900 (2006).
[6] D. Chen, M. White, C. Borries, and B. DeMarco, Phys. Rev. Lett. **106**, 235304 (2011).
[7] S. Trotzky, Y.-A. Chen, A. Flesch, I. P. McCulloch, U. Schollwöck, J. Eisert, and I. Bloch, Nat. Phys. **8**, 325 (2012).
[8] H. Ott, E. de Mirandes, F. Ferlaino, G. Roati, G. Modugno, and M. Inguscio, Phys. Rev. Lett. **92**, 160601 (2004).
[9] C. D. Fertig, K. M. O'Hara, J. H. Huckans, S. L. Rolston, W. D. Phillips, and J. V. Porto, Phys. Rev. Lett. **94**, 120403 (2005).
[10] N. Strohmaier, Y. Takasu, K. Günter, R. Jördens, M. Köhl, H. Moritz, and T. Esslinger, Phys. Rev. Lett. **99**, 220601 (2007).
[11] U. Schneider, L. Hackermüller, J. P. Ronzheimer, S. Will, S. Braun, T. Best, I. Bloch, E. Demler, S. Mandt, D. Rasch, and A. Rosch, Nat. Phys. **8**, 213 (2012).
[12] J.-P. Brantut, J. Meineke, D. Stadler, S. Krinner, and T. Esslinger, Science **337**, 1069 (2012).
[13] M. Gring, M. Kuhnert, T. Langen, T. Kitagawa, B. Rauer, M. Schreitl, I. Mazets, D. A. Smith, E. Demler, and J. Schmiedmayer, Science **337**, 1318 (2012).
[14] M. A. Cazalilla, R. Citro, T. Giamarchi, E. Orignac, and M. Rigol, Rev. Mod. Phys. **83**, 1405 (2011).
[15] B. Paredes, A. Widera, V. Murg, O. Mandel, S. Fölling, I. Cirac, G. Shlyapnikov, T. W. Hänsch, and I. Bloch, Nature (London) **429**, 277 (2004).
[16] T. Kinoshita, T. Wenger, and D. S. Weiss, Science **305**, 1125 (2004).
[17] M. Rigol and A. Muramatsu, Phys. Rev. Lett. **94**, 240403 (2005).
[18] A. Minguzzi and D. M. Gangardt, Phys. Rev. Lett. **94**, 240404 (2005).
[19] M. Rigol and A. Muramatsu, Phys. Rev. Lett. **93**, 230404 (2004).
[20] K. Rodriguez, S. R. Manmana, M. Rigol, R. M. Noack, and A. Muramatsu, New J. Phys. **8**, 169 (2006).
[21] F. Heidrich-Meisner, M. Rigol, A. Muramatsu, A. E. Feiguin, and E. Dagotto, Phys. Rev. A **78**, 013620 (2008).
[22] F. Heidrich-Meisner, S. R. Manmana, M. Rigol, A. Muramatsu, A. E. Feiguin, and E. Dagotto, Phys. Rev. A **80**, 041603 (2009).
[23] D. Muth, D. Petrosyan, and M. Fleischhauer, Phys. Rev. A **85**, 013615 (2012).
[24] J. Kajala, F. Massel, and P. Törmä, Phys. Rev. Lett. **106**, 206401 (2011).
[25] D. Iyer and N. Andrei, Phys. Rev. Lett. **109**, 115304 (2012).
[26] J.-S. Caux and R. M. Konik, Phys. Rev. Lett. **109**, 175301 (2012).
[27] P. Öhberg and L. Santos, Phys. Rev. Lett. **89**, 240402 (2002).
[28] A. del Campo and J. G. Muga, Europhys. Lett. **74**, 965 (2006).
[29] D. Jukić, B. Klajn, and H. Buljan, Phys. Rev. A **79**, 033612 (2009).
[30] M. Jreissaty, J. Carrasquilla, F. A. Wolf, and M. Rigol, Phys. Rev. A **84**, 043610 (2011). Within the Gutzwiller approximation, any Mott insulator is equivalent to a product of local Fock states; see Ref. [2].

[31] J. Wernsdorfer, Ph.D. thesis, Johann Wolfgang Goethe-Universität Frankfurt, 2012.
[32] G. Vidal, Phys. Rev. Lett. **93**, 040502 (2004).
[33] A. J. Daley, C. Kollath, U. Schollwöck, and G. Vidal, J. Stat. Mech. (2004) P04005.
[34] S. R. White and A. E. Feiguin, Phys. Rev. Lett. **93**, 076401 (2004).
[35] S. Will, T. Best, U. Schneider, L. Hackermüller, D.-S. Lühmann, and I. Bloch, Nature (London) **465**, 197 (2010).
[36] See Supplemental Material at http://link.aps.org/supplemental/10.1103/PhysRevLett.110.205301 for details on experimental procedures and t-DMRG calculations.
[37] S. Langer, M. J. A. Schuetz, I. P. McCulloch, U. Schollwöck, and F. Heidrich-Meisner, Phys. Rev. A **85**, 043618 (2012).
[38] M. Polini and G. Vignale, Phys. Rev. Lett. **98**, 266403 (2007).
[39] In the case of a double peak structure [see, e.g., Fig. 1(e)], the HWHM measures half of the distance between the outer edges of the two peaks [36].
[40] The proof for this dynamical symmetry given in Ref. [11] carries over to the bosonic case.
[41] S. Fölling, S. Trotzky, P. Cheinet, M. Feld, R. Saers, A. Widera, T. Müller, and I. Bloch, Nature (London) **448**, 1029 (2007).
[42] T. D. Kühner, S. R. White, and H. Monien, Phys. Rev. B **61**, 12 474 (2000).
[43] M. Cramer, A. Flesch, I. P. McCulloch, U. Schollwöck, and J. Eisert, Phys. Rev. Lett. **101**, 063001 (2008).
[44] The strength of the dipole trap was adjusted as well in order to guarantee a flat potential along the x axis.
[45] M. Rigol, V. Dunjko, and M. Olshanii, Nature (London) **452**, 854 (2008).
[46] I. Hen and M. Rigol, Phys. Rev. Lett. **105**, 180401 (2010).
[47] K. Winkler, G. Thalhammer, F. Lang, R. Grimm, J. H. Denschlag, A. J. Daley, A. Kantian, H. P. Büchler, and P. Zoller, Nature (London) **441**, 853 (2006).
[48] D. Petrosyan, B. Schmidt, J. R. Anglin, and M. Fleischhauer, Phys. Rev. A **76**, 033606 (2007).